

A Machine Learning Method for Prediction of Multipath Channels

Julian Ahrens¹

Lia Ahrens²

Hans D. Schotten³

June 3, 2022

Abstract

In this paper, a machine learning method for predicting the evolution of a mobile communication channel based on a specific type of convolutional neural network is developed and evaluated in a simulated multipath transmission scenario. The simulation and channel estimation are designed to replicate real-world scenarios and common measurements supported by reference signals in modern cellular networks. The capability of the predictor meets the requirements that a deployment of the developed method in a radio resource scheduler of a base station poses. Possible applications of the method are discussed.

Keywords: machine learning, convolutional neural network, multipath transmission, channel estimation, channel prediction

1 Introduction

Today's mobile communication networks are driven by the demand of a steadily increasing number of subscribers for ever higher data rates. This demand has led to the introduction of support for technologies such as millimeter wave transmissions and massive MIMO into the current 5G standard. Apart from the introduction of these new technologies, the available spectrum has to be utilised in the most efficient manner possible. This has already led to the move to orthogonal frequency-division multiple access (OFDMA) and orthogonal frequency-division multiplexing (OFDM) in the fourth-generation mobile broadband standard, which allow for fine grained control over the utilisation of the available radio resources across both the time and frequency domains. While OFDM combats frequency-selective fading by using long symbol times, OFDMA provides further benefits by allowing multiple users to schedule transmission on the subcarriers which are best for them at the time [BS15]. OFDM also allows for different encodings to be used across the available spectrum, thereby giving the scheduler fine grained control over the trade-off transmission data rate vs. signal robustness.

¹Deutsches Forschungszentrum für Künstliche Intelligenz, Julian.Ahrens@dfki.de

²Deutsches Forschungszentrum für Künstliche Intelligenz, Lia.Ahrens@dfki.de

³Deutsches Forschungszentrum für Künstliche Intelligenz, Technische Universität Kaiserslautern, Hans_Dieter.Schotten@dfki.de

The dynamic allocation of radio resources and its scheduling is key to achieving efficient utilisation of the available spectrum. Since base stations manage a large number of transmissions, each across a different channel depending on the position and environment of the individual user equipment (UE), they are natural candidates for hosting an optimisation through dynamic scheduling of the radio resources. To achieve efficient radio resource management, scheduling algorithms need to have information about the current and future states of the transmission channels. In particular, two things are required: On the one hand, a mechanism for the estimation of the transmission channels needs to be in place, i.e., there has to be a measurement of the channel transfer function; on the other hand, the development of the transmission channels over time has to be predicted to allow for estimates of future channel quality.

In LTE systems, channel estimation can be implemented by observing the Cell-Specific Reference Signals (CRS). LTE release 10 (LTE Advanced) supplemented the CRS by the introduction of Channel State Information Reference Signals (CSI-RS). 5G New Radio (NR) does not provide CRS, instead relying exclusively on the flexibly configurable CSI-RS. In this paper, we use a simulation of a multipath propagation transmission channel based on the empirical evidence and the models devised in [COST207]. The channel is estimated by transmitting and measuring a test signal containing a similar amount of information as the LTE CRS. In particular, very similar estimates can be derived from the observation of LTE CRS.

The present work focusses on the aspect of predicting the time-variant transmission channels. A convolutional neural network (CNN) operating on the time-frequency domain and using multiple time resolutions is designed in order to achieve the necessary prediction performance. The proposed CNN is a two-dimensional variant of the WaveNet network architecture proposed in [vdODZ⁺16] and uses dilated kernels on the time axis to achieve the incorporation of multiple time resolutions. A further enhancement to the WaveNet architecture presented here consists in enabling simultaneous multi-step predictions, allowing for the instantaneous predictions of the channel development over a period of 5ms (one half-frame) at a resolution of 500 μ s (one slot) each. This is especially useful, since the allocation of resource blocks can be changed at the half-frame level, necessitating the prediction over at least this time period.

The remainder of this work is structured as follows: Section 2 introduces the simulation from which the transfer functions of a fading channel scenario based on real-world observations are derived. Section 3 describes the employed channel estimation procedure. Section 4 contains the description of the channel predictor which is the essential part of this work. Section 5 summarises the obtained results. In Section 6 we provide a discussion of possible applications and an outlook on future research. Section 7 concludes the paper.

2 Simulation

Setting the position and carrier frequency of the transmitter to $(0,0) \in \mathbb{R}^2$ and $f_{\text{carrier}} = 900\text{MHz}$, respectively, the multipath transmission is simulated by generating 256 scatterers each starting at a randomly chosen initial position

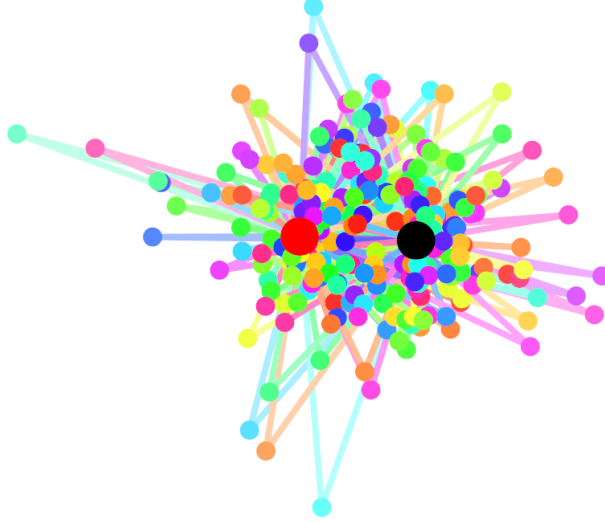


Figure 1: Example configuration of simulation

$(x_0^t, y_0^t) \in \mathbb{R}^2$ such that the power delay profile of the resulting multipath transmission matches the typical urban scenario described in [COST207], and moving at a random time-invariant velocity $(v_x^t, v_y^t) \in \mathbb{R}^2$ with $v_x^t, v_y^t \sim \mathcal{N}(0, \sigma^2)$, $\sigma = 10\text{m/s}$, for $t = 0, \dots, 63$, and $v_x^t, v_y^t = 0$ for $t \geq 64$. The receiver is supposed to move from an initial position $(x_0^*, y_0^*) = (400, 0) \in \mathbb{R}^2$ near the transmitter at velocity $v^* = (v_x^*, v_y^*) \in \mathbb{R}^2$ with $|v^*| = 10\text{m/s}$, $\arctan_2(v_y^*, v_x^*) \sim \mathcal{U}(-\pi, \pi)$ where $\exp(i \arctan_2(y, x)) = (x + iy) / \sqrt{x^2 + y^2}$ for $(x, y) \in \mathbb{R}^2$. The transmissions are assumed to be conducted periodically in blocks. The time for transmitting one block is assumed to be $T = 500\mu\text{s}$ which leads to a discrete time simulation with step size $500\mu\text{s}$. The simulation time amounts to $2^{12} = 4096$ time steps in total. The bandwidth of transmission is set to 12.8MHz . A time interval of length $20\mu\text{s}$ at the beginning of each block is used for the transmission of a test signal generated for the channel estimation. All values are computed and stored using SI base units.

An example configuration of this simulation is shown in Figure 1. The large red and black dots represent the transmitter and receiver, respectively. The smaller dots represent the scatterers which are coloured according to the phase offsets observed on the corresponding transmission paths (shown as lines) with red representing zero offset and cyan representing a phase offset of π .

At each simulation step t and for each ι , the path length reflected by the ι -th scatterer $l_t^{(\iota)} = |(x_t^t, y_t^t) - (0, 0)| + |(x_t^*, y_t^*) - (x_t^t, y_t^t)|$ and its deriva-

tive with respect to time $\frac{d}{dt}l_t^{(\iota)}$ are computed. The corresponding transmission delay time $\sigma_t^{(\iota)}$, the constant phase offset $\theta_t^{(\iota)}$, and the Doppler frequency $f_{D_t}^{(\iota)}$ caused by the ι -th scatterer following the rules $\sigma_t^{(\iota)} = l_t^{(\iota)}/c_0$, $\theta_t^{(\iota)} = ((-l_t^{(\iota)} f_{\text{carrier}}/c_0) \bmod 1) \cdot 2\pi$, and $f_{D_t}^{(\iota)} = -\frac{d}{dt}l_t^{(\iota)} f_{\text{carrier}}/c_0$, respectively, as well as the received signal amplitude $a_t^{(\iota)}$ computed using the free-space propagation model $a_t^{(\iota)} = c_0/(4\pi f_{\text{carrier}} l_t^{(\iota)})$ (cf. [BS15]) are recorded for each scatterer ι . (Here, c_0 refers to the speed of light in vacuum.)

In a setting without line of sight, using linearisation of the phase offset with respect to the Doppler frequency, the time-variant channel impulse response evaluated at time $t + \tau$ for each simulation step t and small τ resulting from the multipath transmission simulated using the above parameters can be approximated by

$$h(\cdot, t + \tau) = \frac{1}{\sqrt{\sum_{\iota=0}^{255} (a_t^{(\iota)})^2}} \sum_{\iota=0}^{255} a_t^{(\iota)} \exp(i\theta_t^{(\iota)} + i2\pi f_{D_t}^{(\iota)} \tau) \delta_{\sigma_t^{(\iota)}}(\cdot).$$

For any signal $\{S_\tau\}_{0 \leq \tau < T}$ being transmitted in the block beginning at time step t through the simulated channel, this consideration leads to a received signal $\{R_\tau\}_{0 \leq \tau < T}$ in the form of

$$\begin{aligned} R_\tau &= (h(\cdot, t + \tau) * S)(\tau) \\ &= \frac{1}{\sqrt{\sum_{\iota=0}^{255} (a_t^{(\iota)})^2}} \sum_{\iota=0}^{255} a_t^{(\iota)} \exp(i\theta_t^{(\iota)} + i2\pi f_{D_t}^{(\iota)} \tau) (\delta_{\sigma_t^{(\iota)}}(\cdot) * S)(\tau). \end{aligned} \quad (1)$$

This parametrisation is used in [Sch88] and delivers a realistic approximation of real-world scenarios for numbers of summands greater than 100 [Kam04]. In order to allow continuous time delays to be applied to discrete time signals, the impulse function $\delta_{\sigma_t^{(\iota)}}(\cdot)$ in (1) is convolved with a windowed sinc(\cdot) function scaled with a given bandwidth. Overall, the channel transmission including pulse shaping with bandwidth restricted to half the sample rate and additive noise is approximated by replacing the $\delta_{\sigma_t^{(\iota)}}(\cdot)$ in (1) by $\sin(\pi(\cdot/2))/(\pi(\cdot/2))\mathbf{1}_{[-8,8]}$ and adding independent and identically distributed Gaussian white noise $\sim \mathcal{N}(0, \sigma^2)$ to the transmitted signal with power σ^2 resulting in a signal-to-noise ratio of 12dB.

3 Channel Estimation

The time-variant channel transfer functions $\mathcal{F}h(\cdot, t + \tau)$ for $t = 0, \dots, 4095T$ and $0 \leq \tau < T$ simulated in Section 2 are approximated by a time series of block wise time-invariant transfer functions $\{\mathcal{F}h^t\}_{t=0, \dots, 4095}$ based on which the estimation and prediction of the channel transmission are conducted. For each transmission block beginning at time step t , in order to estimate the corresponding channel transfer function $\mathcal{F}h^t$, a complex-valued (white noise) test signal $\{\tilde{S}_\tau^t\}_{\tau=0, \dots, N-1}$ whose Fourier transform has constant amplitude and random phases $\sim \mathcal{U}(-\pi, \pi)$ is generated and then transmitted through the channel simulated in Section 2 resulting in a received signal $\{R_\tau^t\}_{\tau=0, \dots, N-1}$.

The transfer function $\mathcal{F}h^t$ is in a first step estimated by

$$\tilde{\mathcal{F}h}^t := \frac{\mathcal{F}R^t}{\mathcal{F}\tilde{S}^t}.$$

Here and in the sequel, $\mathcal{F}X = \{\mathcal{F}X_f\}_{f=0,\dots,N-1}$ refers to the Fourier transform of the respective signal $\{X_\tau\}_{\tau=0,\dots,N-1}$. In order to improve the quality of the preliminary estimator $\tilde{\mathcal{F}h}^t = \{\tilde{\mathcal{F}h}_f^t\}_f$ which is noise corrupted, the corresponding impulse response \tilde{h}^t is windowed by a step function of width $N/2$ and then Fourier transformed, i.e., the estimator $\mathcal{F}\hat{h}^t$ of the channel transfer function is given by

$$\mathcal{F}\hat{h}^t = \mathcal{F}(\mathbf{1}_{[0,N/2]}\mathcal{F}^{-1}\tilde{\mathcal{F}h}^t),$$

where $\mathcal{F}^{-1}Y = \{\mathcal{F}^{-1}Y_\tau\}_{\tau=0,\dots,N-1}$ refers to the inverse Fourier transform of the considered signal $\{Y_f\}_{f=0,\dots,N-1}$ in the frequency domain. The step of windowing the preliminarily estimated impulse response $\tilde{h}^t = \mathcal{F}^{-1}\tilde{\mathcal{F}h}^t$ is conducted due to the observation of a long noisy tail showing up in the recorded \tilde{h}^t which, according to the simulation with maximum transmission delay time less than $N/2$, should be eliminated; this, at the same time, yields a discrete approximation¹ to convolving the estimated channel transfer function with the kernel $\sin(\pi(\cdot/2))/(\pi(\cdot/2))$ so that down sampling with step size 2 (instead of the original step size 1) in the frequency domain delivers an error corrected version of the estimated channel transfer function $\{\mathcal{F}\hat{h}_{2f}^t\}_{f=0,\dots,N/2-1}$.

The initial resolution level of the frequency spectrum is set to $N = 2^9$ which results in an estimated channel transfer function $\mathcal{F}\hat{h}^t$ of length $N/2 = 256$ for each block beginning at simulation step t . Overall, the simulation is run 16 times independently which results in 16 independent time series of the form $\{\mathcal{F}\hat{h}^t\}_{t=0,\dots,4095}$ with $\mathcal{F}\hat{h}^t \in \mathbb{R}^{256}$.

An example realisation of transfer functions estimated during one simulation is shown in Figure 2. The horizontal axis represents time, labelled by time steps t , and the vertical axis represents frequency, labelled by indices of sub-carriers f . Brightness corresponds to amplitude with bright colors representing good signal reception. Colors correspond to phase with red representing phase 0 and cyan representing phase π . One can clearly see the thin dark areas reflecting the effect of frequency selective fading.

In order to ensure that the proposed system could indeed be implemented on current cellular radio equipment, the method of estimation of the simulated channel is chosen in such a manner that the level of channel information obtained is very similar to that commonly available from the reference signals in real-world systems.

4 Channel Prediction

The time series of estimated channel transfer functions from Section 3 are used as labels for training and testing a carefully chosen convolutional neural network (CNN) which delivers one- or multi-step ahead predictions of the time-variant channel transfer functions resulting from the simulation in Section 2. Since additive noise is included in the simulation of the channel, the trained

¹In continuous time, this would be equivalent to convolving with the kernel $\sin(\pi(\cdot/2))/(\pi(\cdot/2))$.

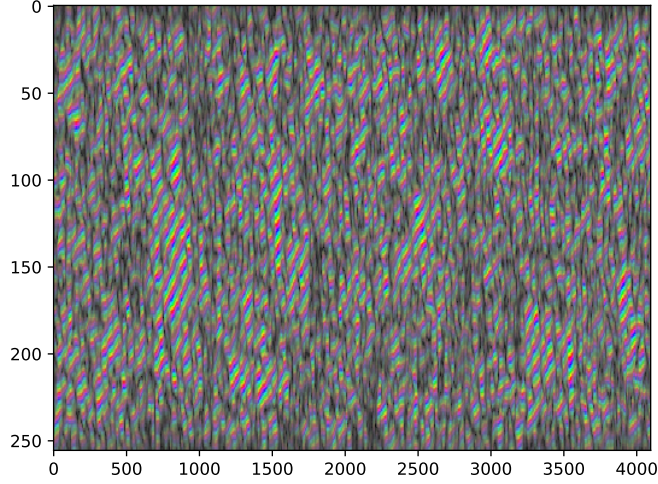


Figure 2: Example plot of estimated transfer functions

neural network also contributes to the denoising of the channel transfer function along with the channel estimation scheme in Section 3.

In general, CNNs are a specific architecture of feed-forward neural networks where linear filters (convolution kernels) instead of traditional single weight parameters are used in a shift invariant manner for the transformation between adjacent layers, making use of local temporal and spatial structure of the input signal within a local receptive field. The local receptive field can be enlarged without the need for increasing the number of parameters by means of the dilation parameter. In the one-dimensional case, a CNN with dilation is known as WaveNet which is introduced in [vdODZ⁺16] for processing audio signals. For more details on CNNs, the readers are referred to [GBC16]. Compared to traditional fully connected neural networks and recurrent neural networks such as LSTMs [HS97], CNNs use fewer parameters and are less receptive to overfitting. In our setting, a two-dimensional convolutional neural network (CNN) with partial dilation is used for building the prediction model which is described in the remainder of this section.

CNNs are a special type of feed-forward neural network made up of one or several convolutional layers. A feedforward neural network is a function mapping an input vector to an output vector making use of a set of parameters which are to be adapted through the training. In a multi-layer neural network, this function operates in the form of several such functions in succession each transforming the corresponding input vector into an output vector. In our setting for processing the time series of channel transfer functions $\{\mathcal{F}\hat{h}^t\}_{t=0,1,\dots}$ with $\mathcal{F}\hat{h}^t \in \mathbb{R}^{256}$, we use two-dimensional convolutional layers where each input vector is indexed with three axes related to the real-or-imaginary part of the complex plane, the simulation time steps, and the frequency domain, and the transformation is conducted by convolving the input vector with a convolution kernel made up of free parameters to be adapted and adding a free parameter

vector called bias to the result. For our purpose of multi-step prediction, we also consider the evolution of the time series over a long period of time, for which we use the so-called dilation parameter on the time axis defining the spacing between the free parameters in the convolution kernel. The introduction of the dilation parameter enables us to extend the receptive field of the CNN in time without taking extra parameters for fitting.

For delivering at most m -step ahead predictions of the future channel transfer function, we use a 5-layer CNN beginning with 4 consecutive partially dilated convolutional layers along the t -axis with channel sizes 2, 6, 12, 12, 6, followed by one convolutional layer with $2m$ output channels. In each partially dilated convolutional layer, the size of the free convolutional kernel is set to (4, 5) for the time and frequency axis, respectively, and the dilation parameter is defined by 4 to the power of the corresponding layer number. The final layer is endowed with 1×1 -convolution kernels. Apart from the last layer, the hyperbolic tangent is used as activation function in each layer. In order to improve the back propagation of the gradient (cf. [RHW86]), a residual convolutional layer (cf. [HZRS16]) with kernel size (1, 1) is added to each partially dilated convolutional layer. The above layout is common in convolutional neural networks and is designed to best adapt to our task and the nature of the input signals.

During the training, the free parameters in our CNN are adjusted to the labelled training data by minimising the mean squared error of prediction along the negative direction of the gradient of the error function with respect to the parameters, for which we use a refined version of stochastic gradient descent (SGD) called ADAM training algorithm (cf. [KB15] for more details). The gradient for each update is computed by means of the so-called backpropagation algorithm (cf. [RHW86]) based on the chain rule.

In our setting, the 16 independent time series of channel transfer functions $\{\mathcal{F}\hat{h}^t\}_{t=0,\dots,4095}$ with $\mathcal{F}\hat{h}^t \in \mathbb{R}^{256}$ are each divided into 8 segments which are to be fed into the CNN as input vectors and grouped as training, validation, and test parts with the proportion 6 : 1 : 1. The ADAM optimiser with learning rate $\gamma = 0.01$ is run for 30 training epochs in total.

5 Results

The performance of our approach to delivering multi-step ahead prediction is measured in a setting with $m = 10$ for training the corresponding CNN to output 10-step ahead predictions at most. The mean squared errors (MSEs) are evaluated for training, validation, and test data which are presented on the left of Table 1. The similarity of performance evaluated on all three subdatasets indicates no significant overfitting.

As a baseline, we consider the trivial prediction where all future values of the time series are set to the latest observed value; the MSE of such a prediction scheme provides a measure for the variation of the underlying time series over time and is displayed on the right of Table 1. Overall, the instantaneous long-term prediction with our CNN using $m = 10$ facilitated by employing the dilation parameter in time delivers much more accurate results than the trivial prediction scheme. Moreover, the iterative prediction scheme for long-term

Table 1: MSE for prediction length Δt from 1 to 10

Δt	Training	Validation	Test	Trivial
1	0.1466	0.1460	0.1424	0.2217
2	0.1579	0.1569	0.1538	0.2532
3	0.1753	0.1735	0.1707	0.3047
4	0.2014	0.1988	0.1962	0.3750
5	0.2357	0.2321	0.2298	0.4621
6	0.2757	0.2723	0.2704	0.5644
7	0.3249	0.3208	0.3183	0.6788
8	0.3821	0.3763	0.3735	0.8040
9	0.4459	0.4393	0.4354	0.9382
10	0.5133	0.5055	0.5005	1.0797

predictions is considerably computation-time consuming, which highlights the efficiency of our instantaneous long-term prediction.

In Figures 3, 4, 5, and 6, the power density spectra in dB of an example channel transfer function evaluated at time steps t_0 and $t_0 + \Delta t$ and the Δt -step ahead instantaneous prediction for time $t_0 + \Delta t$, $\Delta t = 1, 2, 5, 10$, output by the trained CNN with $m = 10$ are plotted in blue, yellow, and green, respectively. Notice in particular that most of the negative peaks of the future power density spectra are correctly detected by the predictor, which suggests the utility of our approach in handling situations with frequency selective fading in an OFDM transmission scheme (see Section 6 for more discussion).

6 Discussion

As mentioned in the introduction, the method proposed in the preceding sections can be employed to provide an OFDMA/OFDM radio resource scheduler located in a base station with predictions necessary for an efficient scheduling of radio resources. There are two main aspects of the scheduler which can benefit from this information:

Firstly, the predictions can be used to decide to which user a specific radio resource element should be allocated by estimating the relative usefulness of assigning the element to a specific user compared to the utility another user may have of it. For instance, consider the case where two radio resource blocks RRB A and RRB B are assigned to users UE A and UE B, respectively. If the predictor predicts that during the next half-frame the part of the spectrum on which RRB A is transmitted will become faded for UE A, but a strong signal could be received by UE B, it would be advantageous to change the allocation and assign RRB B to UE A and RRB A to UE B.

The other aspect is that the scheduler may control the choice of encoding used on each of the radio resource elements. In particular, if a prediction reveals that a certain part of the spectrum will become faded for a particular user and a reallocation among the users as in the case discussed previously is not applicable, the scheduler may initiate a change of the employed encoding, for instance from 64QAM down to 16QAM, thereby increasing the robustness of the signal and counteracting the decreasing signal-to-noise ratio. In ex-

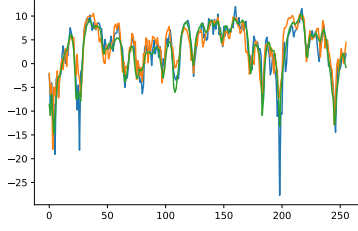


Figure 3: Power density spectrum in dB for $\Delta t = 1$

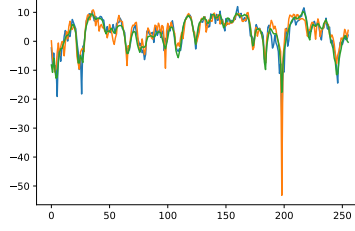


Figure 4: Power density spectrum in dB for $\Delta t = 2$

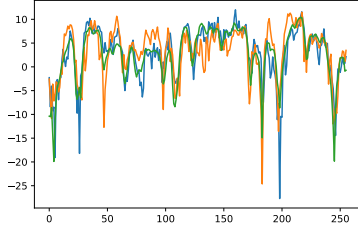


Figure 5: Power density spectrum in dB for $\Delta t = 5$

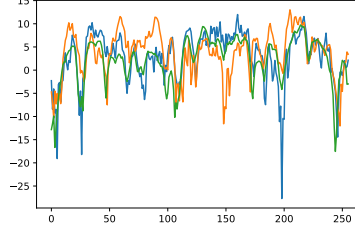


Figure 6: Power density spectrum in dB for $\Delta t = 10$

trema cases of frequency selective fading, transmissions on the corresponding frequencies could even be disabled completely.

In future research, we hope to expand on both of these topics by developing an adaptive coding scheme and a dynamic scheduler for the multi-user case based on the research performed in this article.

7 Conclusion

In this paper, we simulated a multipath transmission scenario, implemented a channel estimation scheme, and designed a machine learning model for predicting the resulting channel transfer functions over multiple time steps. Our results show that the machine learning model is capable of capturing characteristics of the evolution of the channel and provides reasonable predictions. We addressed possible applications of the method in real-world systems which we plan to implement and evaluate in future research.

Bibliography

- [BS15] Cory Beard and William Stallings. *Wireless Communication Networks and Systems, Global Edition*. Pearson, 2015.

- [COST207] COST 207 Management Committee. COST 207 Digital land mobile radio communications. Technical report, Commission of the European Communities, 1990.
- [GBC16] Ian Goodfellow, Yoshua Bengio, and Aaron Courville. *Deep Learning*. MIT Press, 2016. <http://www.deeplearningbook.org>.
- [HS97] Sepp Hochreiter and Jürgen Schmidhuber. Long Short-Term Memory. *Neural Computation*, 9(8):1735–1780, 1997. doi:10.1162/neco.1997.9.8.1735.
- [HZRS16] Kaiming He, Xiangyu Zhang, Shaoqing Ren, and Jian Sun. Deep residual learning for image recognition. In *Proceedings of the 29th IEEE Conference on Computer Vision and Pattern Recognition, CVPR 2016*, Las Vegas, NV, USA, 2016. doi:10.1109/CVPR.2016.90, arXiv:1512.03385 [cs.CV].
- [Kam04] Karl-Dirk Kammeyer. *Nachrichtenübertragung*. Informationstechnik. Vieweg+Teubner Verlag, third edition, 2004. doi:10.1007/978-3-322-94062-9.
- [KB15] Diederik P. Kingma and Jimmy Lei Ba. Adam: A method for stochastic optimization. In *Proceedings of the 3rd International Conference on Learning Representations, ICLR 2015*, San Diego, CA, USA, 2015. arXiv:1412.6980 [cs.LG].
- [RHW86] David E. Rumelhart, Geoffrey E. Hinton, and Ronald J. Williams. Learning representations by back-propagating errors. *Nature*, 323:533–536, 1986. doi:10.1038/323533a0.
- [Sch88] Henrik Schulze. Stochastische Modelle und digitale Simulation von Mobilfunkkanälen. In *Kleinheubacher Berichte*, volume 32, pages 473–483, 1988.
- [vdODZ⁺16] Aaron van den Oord, Sander Dieleman, Heiga Zen, Karen Simonyan, Oriol Vinyals, Alex Graves, Nal Kalchbrenner, Andrew Senior, and Koray Kavukcuoglu. WaveNet: A generative model for raw audio. *arXiv e-prints*, 2016. arXiv:1609.03499 [cs.SD].